Available online at www.sciencedirect.com

ScienceDirect

Procedia CIRP 31 (2015) 369 – 374

www.elsevier.com/locate/procedia

15th CIRP Conference on Modelling of Machining Operations

Discrete Element Modelling of Drag Finishing

Eckart Uhlmann[a], Alexander Eulitz[a]*, Arne Dethlefs[a]

[a]*Technische Universität Berlin, Institute for Machine Tools and Factory Management, Berlin, Germany*

* Corresponding author. Tel.: +49-30-314-24963; fax: +49-30-314-25895. E-mail address: eulitz@iwf.tu-berlin.de

Abstract

Drag finishing is a machining process that is used to improve the surface topology of workpieces. Workpieces are moved through a bulk of differently shaped abrasives, the so called media. Material removal is caused by the relative motion between workpiece and media. The material removal rate is mainly depending on the contact intensity between workpiece and media. Up to now there is no viable way to determine the intensity of single contacts empirically. However, a sound understanding of single contacts with respect to impact forces and velocities could greatly improve process comprehension and reduce trial and error process design efforts. For that reason the movement of media and workpiece is modelled using the Discrete Element Method (DEM). In this paper a comprehensive approach is presented covering formulation, calibration, validation and utilization of the DEM. Media is considered as an aggregation of elastic particles that are subject to contact, damping and gravitational forces causing particle movement. Geometric boundary conditions, i.e. workpiece and drag finishing bowl, are implemented as elastic facets. Contact forces are calculated according to a non-linear, simplified Hertz-Mindlin contact force model. Energy is dissipated by viscous damping and friction at contacts. Necessary parameters of the model are determined experimentally. The validation of the model's behaviour shows good agreement with experimental data. Finally the model is used to determine local contact intensities on the workpiece surface and between particles. By analysing simulated contact forces, the formation of dominant contact chains between particles is observed and investigated.

Peer-review under responsibility of the International Scientific Committee of the "15th Conference on Modelling of Machining Operations

Keywords: Finishing; Modelling; Discrete Element Method (DEM)

1. Introduction

Drag finishing is a versatile machining process that is used to improve the surface topology of workpieces. These are moved in a bulk of abrasives, the so called media. Caused by the relative motion of workpiece and media, material of the workpiece is removed. In contrast to other mass finishing processes, like vibratory or centrifugal disc finishing, workpieces are fixed by a clamping device and media is not agitated in drag finishing. Industrial drag finishing processes are usually carried out with a fixed track setup that guides the workpieces through the media on a set or only slightly adaptable trajectory. A major benefit of the fixed workpiece setup is that workpieces cannot collide. Typical applications of drag finishing include medical implants, gear components, turbine blades or rounding of cutting tool edges [1,2,3]. A newly developed and patented setup is robot guided drag finishing [4], where an industrial 6-axes robot is used to guide workpieces through media, resulting in versatile trajectories and precise setting of workpiece velocities [5]. By increasing workpiece velocities higher pressure than in vibratory finishing processes can be achieved resulting in increasing material removal rates and quicker processing. In addition the defined trajectories of the workpieces allow for enhanced machining of certain features at complex workpieces.

A lot of researchers have presented models for mass finishing processes so far. Most of them are descriptive models for vibratory finishing that correlate process parameters with surface quality for certain workpieces. MATSUNAGA [6] investigated contact mechanisms and velocity fields in vibratory finishing, but did not establish a correlation between processing results and measured or observed process characteristics. Additionally HASHIMOTOS findings [7] are of high relevance to the field of mass

Peer-review under responsibility of the International Scientific Committee of the "15th Conference on Modelling of Machining Operations
doi:10.1016/j.procir.2015.03.021

finishing. Based on empirical studies he established basic rules for mass finishing processes that were confirmed in large parts by a recent investigation of UHLMANN ET AL. [8]. SPELT'S group [9,10,11,12,13] established a correlation between process forces, contact mechanisms and reachable surface quality in vibratory finishing. An important finding of SPELT'S group is the identification of three major contact modes that occur when spherical media is used in vibratory finishing: single impact, free rolling of single spheres and rolling of spheres in packages [13].

Nomenclature

α	empirical constant
c_n	damping coefficient in normal direction
c_t	damping coefficient in tangential direction
d_s	submersion depth
e_n	coefficient of restitution in normal direction
e_t	coefficient of restitution in tangential direction
E	Young's modulus
F_n	normal force
F_t	tangential force
G	shear modulus
h_f	height of filling
k_n	contact stiffness in normal direction
k_t	contact stiffness in tangential direction
μ_{ij}	friction coefficient of material combination i, j
m	mass
n_b	number of balls
R_b	radius of balls
R_i	radius of particle i
ρ_i	density of material i
δ_n	displacement in tangential direction
δ_t	displacement in normal direction
$\Delta\tau$	time step
t_p	process time
ν_i	Poisson's ratio of material i
v_t	contact tangential velocity
v_w	workpiece velocity

The significance of contact forces and mechanisms in mass finishing processes has been emphasized by many researchers [9,14,15,16]. It has been shown that contact forces and impact velocities have great influence on process outcome in terms of material removal, roughness and hardness of the workpiece. As a consequence there have been many investigations on how to measure forces and impact velocities on the workpiece. Most of them make use of in situ measurement of contact forces. Costly measurement devices with high sampling rates have to be used to record maximum impact forces [9]. Furthermore a major handicap of this approach is the dependence of force magnitudes on sensor surface compliance [9,17]. CIAMPINI ET AL. [14] proposed to extract normal impact velocity from measured forces instead. Based on the determined impact velocities, energy imparted to arbitrary workpieces can be inferred, disregarding compliances. Nevertheless forces have to be measured for all considered machine settings and workpiece geometries. Directly obtaining impact velocities in mass finishing processes is also challenging, as measuring devices have to be placed appropriately in the bulk media. HASHEMNIA ET AL. [18] have developed a laser displacement probe that is able to measure impact and bulk flow velocities in vibrationally fluidized beds. Other reported approaches concentrate on measuring workpiece or bulk flow velocity, e. g. using spatial and time-based analyses of photographs [19]. Instead of force or velocity based approaches CIAMPINI ET AL. [11] used an almen strip system, common in shot peening applications, to characterise the effect of different process parameters on the aggressiveness of a vibratory finishing process. Having simulated the occurring impacts with an electromagnetic apparatus they found that normal impacts are dominating in vibratory finishing. Because in situ force and impact velocity measurement is a complex task susceptible to disturbances in the measuring chain, a different approach is presented, that allows for modelling of contact intensities for arbitrary workpiece geometries and materials using the Discrete Element Method (DEM).

Up to now results from two different approaches towards a deterministic numerical process model for mass finishing have been reported:

- Modelling of the motion of spherical media with the DEM [20,21,22,23,24]
- Modelling of the media's velocity fields using Computational Fluid Dynamics (CFD) for centrifugal disk finishing [19] and vibratory finishing of immobilized cylinders [25]

Notably, only CARIAPA [19] and UHLMANN ET AL. [20] look at the three-dimensional movement of abrasive media in their models. All other approaches consider mass finishing processes with spherical steel or glass media or are restricted to two dimensions. CARIAPA'S approach allows for a qualitative prediction of material removal. The work of UHLMANN ET AL. on a comprehensive process model [20] combines an empirical geometry based model for surface roughness prediction [8] with contact intensity simulation using DEM. Using this comprehensive process model a quantitative prediction of material removal and roughness should be possible.

2. Discrete Element Method (DEM)

In the following a model to numerically simulate contacts between abrasive media and workpieces using DEM will be presented. The goal is to simulate the number, type and intensity of contacts between workpieces and abrasive media for finite areas of any workpiece. The DEM-model is used to simulate a small-scale drag finishing process. Findings from the model are utilized to broaden process comprehension.

The approach presented in this paper is based on the work of UHLMANN ET AL. [8], in which bulk motion is modelled using the open source framework Yade [26]. Media is considered as a bulk of discrete, elastic, spherical particles that overlap depending on contact forces, the so called soft-particle approach. In contrast to the hard-particle approach, that is based on instantaneous exchange of momentum when contact occurs, the soft-particle approach allows for multiple

particle contacts, which are common for dense granular media, at the cost of smaller time steps, resulting in higher computation times [27]. Most soft-particle models make use of an artificial increase in time step by allowing softer interaction. This is usually done by setting particle stiffnesses lower than physically observable [28].

Geometric boundary conditions, i. e. bowl and workpieces, are implemented as facets. As a first step, spherical media is considered. In that case only point-contacts occur, which reduces the effort for collision detection and contact calculation considerably. In order to simulate the number, type and intensity of contacts for finite areas of any workpiece, a suitable model for particle-particle and particle-facet contacts has to be chosen. This is presented in the next section.

3. Model formulation

In the presented approach, contact forces between two bodies are calculated according to the non-linear viscoelastic simplified Hertz-Mindlin contact force model, see Fig. 1. It is generally accepted that the Hertz-Mindlin contact force model is suitable to model contact between two elastic spheres or one sphere and a half space [29,30].

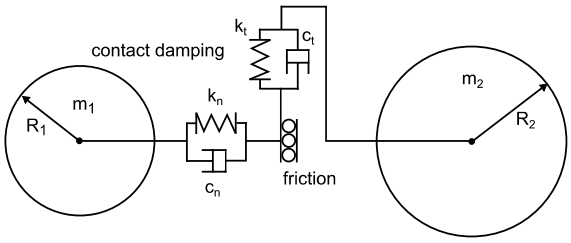

Fig. 1. Spring dash-pot slider contact model for two spheres in contact.

The model is based on Hertzian contact equations [31] in normal direction and the Mindlin no-slip approach [32,33] in tangential direction. The non-linear correlation between normal force F_n and normal displacement δ_n is given by

$$F_n = k_n \delta_n^{3/2}. \tag{1}$$

Contact stiffness k_n is expressed by

$$k_n = \frac{4}{3} E_{eq} \sqrt{R_{eq}}, \tag{2}$$

where E_{eq} is the equivalent Young's modulus expressed by

$$\frac{1}{E_{eq}} = \frac{1-\nu_1^2}{E_1} + \frac{1-\nu_2^2}{E_2}, \tag{3}$$

with E_1 and E_2 being the Young's moduli and ν_1 and ν_2 Poisson ratios of particles in contact. R_{eq} is the equivalent radius of the contact which is given by

$$\frac{1}{R_{eq}} = \frac{1}{R_1} + \frac{1}{R_2}, \tag{4}$$

where R_1 and R_2 are radii of particles in contact. According to MINDLIN [32] and MINDLIN AND DERESIEWICZ [33] the relation between the tangential force F_t and tangential displacement δ_t is depending on the normal displacement δ_n. They proposed equations that constitute this relationship for several contact configurations. If a contact surface is allowed to slip, equations become complicated because the history of the contact has to be considered. To reduce computing time a non-slipping contact surface is assumed in this paper. I. e. the equation for tangential contact stiffness k_t is given by

$$k_t = 4\sqrt{R_{eq}} \frac{G_m}{2-\nu_m} \delta_n, \tag{5}$$

where G_m is the mean shear modulus and ν_m is the mean Poisson's ratio of the particles in contact. In general shear modulus G can be expressed by

$$G = \frac{E}{2(1+\nu)}. \tag{6}$$

Note that tangential contact stiffness k_t is a function of the normal displacement δ_n. In Yade, tangential contact force F_t is calculated incrementally by

$$F_t = F_{t,\tau-1} - k_t \mathrm{v}_t \Delta\tau, \tag{7}$$

where $F_{t,\tau-1}$ is the tangential contact force at the previous time step, v_t is the contact tangential velocity and $\Delta\tau$ is the time step.

3.1. Damping

Energy of the particulate media in the system is dissipated through friction and viscous damping at the contacts. Force transmitted in tangential direction between two particles is limited by the Mohr-Coulomb friction law. It should be noted that in the original DEM-formulation by CUNDALL AND STRACK [34] a global damping was introduced. I. e. damping forces were part of the equations of motions. This does not represent a physical phenomenon but is an artificial numerical damping. In this work non-linear viscous damping at the contacts (also known as local damping), represented by the dash-pots in Fig. 1, is used. It has been shown by ZHANG AND WHITEN [35] that non-linear contact damping is more suitable to resemble experimental results than linear contact damping. Damping force in normal direction $F_{n,d}$ is calculated by

$$F_{n,d} = c_n(\delta_n) v_n, \tag{8}$$

where the damping coefficient c_n is a function of normal displacement δ_n. TSUJI ET AL. [36] derived a formulation for the damping coefficient c_n

$$c_n(\delta_n) = \alpha\sqrt{m_{eq}k_n}\,\delta_n^{1/4}, \tag{9}$$

where α is an empirical constant related to the coefficient of restitution in normal direction e_n and m_{eq} is the equivalent mass, calculated in analogous manner as (4). ANTYPOV AND ELLIOTT [37] mapped the Hertzian contact model onto the linear spring dash-pot model. They provided an analytical relationship between the empirical constant α from (9) and the coefficient of restitution in normal direction e_n, i. e.

$$\alpha(e_n) = \frac{-\sqrt{5}\log(e_n)}{\sqrt{\log^2(e_n)+\pi^2}}. \tag{10}$$

Conforming to the work of TSUJI ET AL. [36] the damping coefficient in tangential direction c_t is assumed to be equal to the damping coefficient in normal direction c_n.

4. Model setup

A large number of abrasive particles are used in usual drag finishing processes, see Fig. 2a. This results in immense calculation times for setups modelled exactly according to these processes. For that reason a smaller bowl and rod are considered as a first step, see Fig. 2b. This reduces the number of particles to 1422. Geometric boundary conditions of the modelled setup can be found in Fig. 3.

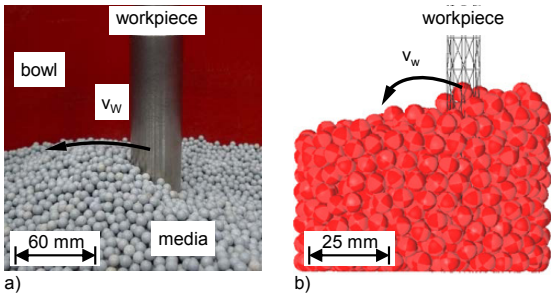

Fig. 2. Drag finishing setup (a) real process, (b) DEM-model.

Calibration approaches for modelling of granular material can roughly be divided into two groups: physical and phenomenological approaches. In physical calibration approaches, direct correlations between model parameters and experimental results are used to calibrate the model. Thus model parameters are determined on a per-particle base (micro-scale) according to well-known mechanical relationships. Typical setups comprise sphere drop, tensile or compression tests [38,39]. Because bulk materials often consist of randomly shaped particles, physical calibration is not always feasible. In such cases, phenomenological calibration, which is focused on the macro-scale bulk behaviour of particles, can be used [30]. Thereby, model parameters are varied until certain macroscopic behaviour of granular media is observed. Hereby particle stiffness is usually set at considerably lower values than real stiffness, resulting in larger time steps and hence faster calculation [27,38]. By calibrating the bulk behaviour of soft particles it is supposed that, disregarding unrealistic stiffnesses, simulation results can be transferred to real granular media. Examples for corresponding calibration experiments are triaxial tests, shear tests and bulk compression tests. If micro-scale behaviour, e. g. magnitude of contact forces, is of interest, as it is the case for modelling of drag finishing, physical calibration is necessary.

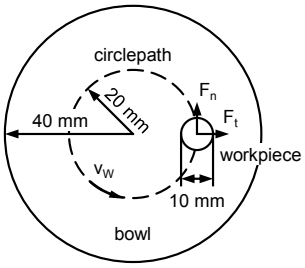

Fig. 3. Geometries of modelled small-scale process.

The input parameters for the contact model are Young's modulus E_i, Poisson's ratio ν_i, density ρ_i, coefficient of restitution in normal direction e_n and friction coefficient μ_{ij} for all materials i and material combinations i, j ($i, j \in M$, $i \neq j$ with number of materials M).

Young's modulus E_c of the spherical ceramic-bond media that was used for this paper was determined by considering the media as a multiphase material. Using micro indentation tests and photo analyses of microscope images of cross-section polished media, Young's moduli of the single phases were calculated. The overall Young's modulus of media was estimated at $E_c = 77$ GPa, the overall Poisson ratio at $\nu_c = 0.19$, respectively, both using the approaches presented by HASHIN AND SHTRIKMAN [40] and ONDRACEK [41]. Friction coefficients μ_{ij} for all material combinations were obtained in a scratch test, i. e. the friction coefficient for ceramic sphere scratching on another one $\mu_{cc} = 0.34$ and ceramic sphere scratching on a bearing steel (1.3505) plate $\mu_{cs} = 0.28$. The density of the ceramic media was determined at $\rho_c = 2656$ kg/m³, for bearing steel (1.3505) it was taken from a data sheet with $\rho_s = 7610$ kg/m³.

Damping behaviour of colliding particles is often investigated using a sphere drop setup [29,39]. In this paper the coefficient of restitution in normal direction e_n is determined by iteratively comparing experimental with simulated forces for varying coefficients of restitution in normal direction e_n in simulation. This means, a sphere (ceramic-bond media FSG 6MM BALLS, Walther Trowal) which is released from a height of 10 mm hits a horizontal plate (bearing steel 1.3505), that is mounted on a force sensor, multiple times. For the calibration of the damping behaviour the first three impacts are considered. The change in the magnitude of the maximum impact forces and the time since the first impact were used to fit the coefficient of restitution in normal direction e_n. Doing so a coefficient of restitution in normal direction for ceramic-steel contact $e_{n,cs} = 0.68$ was estimated. Due to FSG media is not available as a plate the coefficient of restitution in normal direction for ceramic-ceramic contact $e_{n,cc}$ could not be determined with the described setup. Instead it is taken from similar investigations done by KUMAR AND SATHYAN [39] who obtained $e_{n,cc} = 0.86$.

5. Validation

The model was verified using the described small-scale bowl that was filled with ceramic media and an exemplary set of process parameters. In the experimental setup, the total force acting on the workpiece during a drag finishing process was measured using a KISTLER model 9273 dynamometer. Normal force F_n from the experiment is shown in Fig. 4a. The mean experimental normal force is $F_{n,exp,mean} = -2.59\ N \pm 0.66\ N$ (± indicates standard deviation). The base level of the force is caused by static bulk pressure. In addition there are some peculiar peaks of the normal force F_n, e. g. at process times $t_p = 6.250$; 10.055 s.

In the simulation the total force acting on the rod is measured in a workpiece aligned coordinate system, i. e. normal force F_n is always pointing in the direction of the workpiece velocities v_w and the tangential force F_t is perpendicular to it, see Fig. 3. Fig. 4a shows the total simulated forces in normal and tangential direction with spherical ceramic media and a steel rod for one revolution of the workpiece for a small scale process with geometries as described in Fig. 3. For simplicity reasons bowl and rod are made of the same material. This reduces the number of occurring material combinations which results in less parameters that have to be determined experimentally beforehand. Mean simulated normal force is $F_{n,sim,mean} = -1.99\ N \pm 0.63\ N$, i. e. it deviates from the mean experimental normal force by about 23.17 %. However, simulated forces show comparable amplitudes and variation as well as some distinct peaks as it was the case for experimental forces. Using new means of contact intensity analysis, the so called interaction network, it can be shown that these peaks are caused by the formation of contact chains. In Fig. 4b-c interaction networks after 4.5 s of process time are shown. They are coloured according to the magnitude of the normal contact force of the corresponding interaction, ranging from green for no contact force to red for highest overall contact force. The radius of each cylinder is also scaled by normal contact force, i. e. the cylinder of the interaction with the maximum contact force has a radius equal to the mean radius of the balls $R_b = 3.27$ mm whereas cylinders of interactions with lower contact forces have smaller radii. It can be seen that contact forces in direction of workpiece velocity v_W are considerably higher than in other directions. Furthermore in the region behind the workpiece the smallest contact forces can be observed. Interestingly the active zone inside the bulk reaches far ahead of the workpiece. Additionally, Fig. 4b confirms that contact forces tend to increase with depth, as expected because of the increasing pressure caused by the weight of media.

The most important finding from Fig. 4b-c is the formation of dominant contact chains between rod and bowl. Contact chains with comparable orientations in xy-plane, see Fig. 4b, were observed after various process times and typically go in hand with distinct peaks in simulated normal forces. The altitude in the bowl and orientation in xz-plane varies, see Fig. 4c. This phenomenon will be subject to further investigations, in which a correlation with known contact mechanisms will be checked. First analyses of microscope pictures reveal that on some workpiece surfaces deep scratches can be found on regions pointing in the direction of the bowls boundary. This is considered as a first indication for presence of contact chains. It is noted that further efforts have to be made using other process parameter sets for validation.

Model setup:		Density:	
Submersion depth:		ρ_c = 2656	kg/m³
d_s = 50	mm	ρ_s = 7610	kg/m³
Workpiece velocity:		Young's Modulus:	
v_w = 0.01	m/s	E_c = 77	GPa
Radius of balls:		E_s = 210	GPa
R_b = 3.27	mm	Friction coefficient:	
δ_b = 0.15	mm	μ_{cs} = 0.28	
Number of balls:		μ_{cc} = 0.34	
n_b = 1422		Poisson's number:	
Height of filling:		ν_c = 0.19	
h_f = 70	mm	ν_s = 0.30	
Contact law and parameters:		Coefficient of restitution (COR):	
Hertz-Mindlin no-slip,		$e_{n,cc} = e_{t,cc}$ = 0.86	
viscous damping		$e_{n,cs} = e_{t,cs}$ = 0.68	

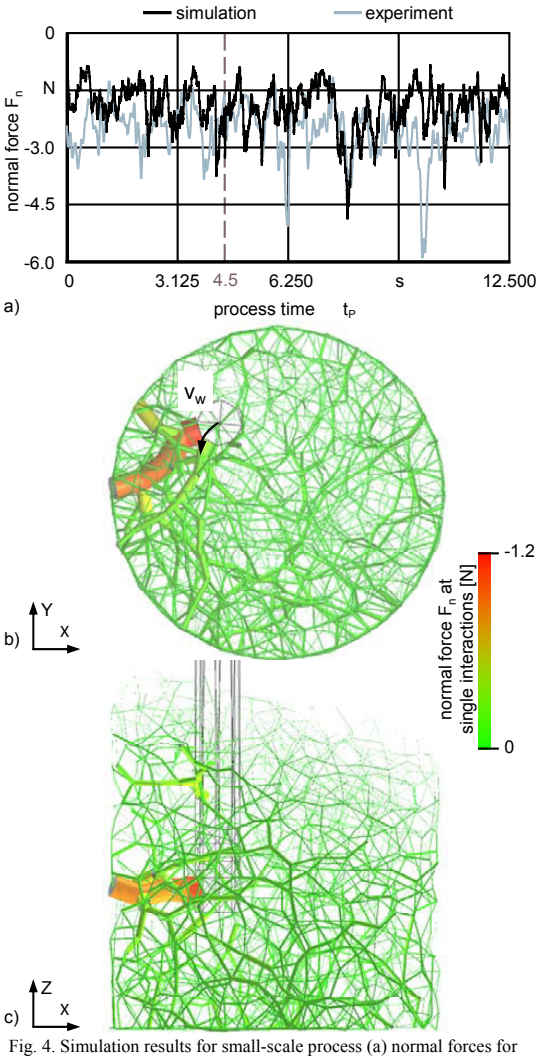

Fig. 4. Simulation results for small-scale process (a) normal forces for simulation and experiment (b, c) interaction networks.

6. Conclusion and outlook

After validation of the presented model, it was shown, how such a model can be used to broaden the understanding of process fundamentals. For the first time contact chains were identified by the evaluation of interaction networks. Now it is possible to determine the number, type and intensity of contacts between workpieces and abrasive media for finite areas of any workpiece. This will be subject to further investigations. As a next step several tests consisting of single and multi-contact, quasi-static and dynamic scenarios will be carried out, in which forces, measured in experiments and calculated in simulations will be compared. Furthermore the laser displacement probe introduced by HASHEMNIA ET AL. [18] could be used to validate DEM predictions of impact velocities on the workpiece surface. Finally contact intensities calculated with the DEM-model described in this paper should be linked to the output of the material removal model, mentioned above [8,20], thus creating a comprehensive process model.

Acknowledgements

This work is supported by the German Research Foundation (DFG), project UH 100/180-1.

References

[1] Gillespie L K. Mass Finishing Handbook. 1st ed. New York: Industrial Press; 2007.
[2] Holzknecht E. Drag Finishing Displaces Manual And Robotic Grinding & Polishinig. MFN Metal Finishing News 2014:42-4.
[3] Risse K. Einflüsse von Werkzeugdurchmesser und Schneidkanten-verrundung beim Bohren mit Wendelbohrern in Stahl, Berichte aus der Produktionstechnik, Aachen: Shaker; 2006;15.
[4] Uhlmann E, Hasper G, Mihotovic V, Fraunhofer Gesellschaft, TU Berlin, Verfahren und Vorrichtung zum Gleitspanen eines Werkstücks; Patent DE 10 2009 024 313; 2011.
[5] Uhlmann E, Dethlefs A. Polieren komplexer Bauteile. WB Werkstatt + Betrieb 2011;6:2831.
[6] Matsunaga M, Hagiuda Y. Researches on barrel finishing. Report of the Institute of Industrial Science, Tokyo: The University of Tokyo 1967;17:107-55.
[7] Hashimoto F. Modelling and Optimization of Vibratory Finishing Process. Annals CIRP 1996;45:303-6.
[8] Uhlmann E, Dethlefs A, Eulitz A. Investigation into a geometry-based model for surface roughness prediction in vibratory finishing processes. Int J Adv Manuf Technol 2014;75:815-23.
[9] Wang S, Timsit RS; Spelt JK. Experimental investigation of vibratory finishing of aluminum. Wear 2000;243:147-56.
[10] Ciampini D. Impact Velocity, Almen Strip Curvature and Residual Stress Modelling in VibratoryFinishing. Toronto: University of Toronto; 2008.
[11] Ciampini D, Papini M, Spelt JK. Characterization of vibratory finishing using the Almen system. Wear 2008;7-8:671-8.
[12] Ciampini D, Papini M, Spelt JK. Modeling the development of Almen strip curvature in vibratory finishing. J Mat Proc Technol 2009;6:2923-39.
[13] Yabuki A, Baghbanan MR, Spelt JK. Contact forces and mechanisms in a vibratory finisher. Wear 2002;252:635-43.
[14] Ciampini D, Papini M, Spelt JK. Impact velocity measurement of media in a vibratory finisher. J Mat Proc Technol 2007;2-3:347-57.
[15] Kumar PP, Sathyan S. Simulation of 1D Abrasive Vibratory Finishing Process. Adv Mat Res 2012;565:290-5.
[16] Baghbanan MR, Yabuki A, Timsit RS, Spelt JK. Tribological behavior of aluminum alloys in a vibratory finishing process. Wear 2003;7-12:1369-79.
[17] Johnson KL, Contact Mechanics, Cambridge: Cambridge University Press 1985:363-5.
[18] Hashemnia K, Mohajerani A, Spelt JK. Development of a laser displacement probe to measure particle impact velocities in vibrationally fluidized granular flows. Powder Technol 2013;235:940-52.
[19] Cariapa V, Park H, Kim J, Cheng C, Evaristo A. Development of a metal removal model using spherical ceramic media in a centrifugal disk mass finishing machine. Int J Adv Manuf Technol 2008;1-2:92-106.
[20] Uhlmann E, Dethlefs A, Eulitz A. Investigation of Material Removal and Surface Topography Formation in Vibratory Finishing. Procedia CIRP 2014;14:25-30.
[21] Kawamoto Y, Kataoka M, Uekusa M, Terumichi Y. Behavior of Two Kinds of Particles in Rotary Barrel with Planetary Rotation. Multibody Sys Dyn 2004;3:187-207.
[22] Naeini SE, Spelt JK. Two-dimensional discrete element modeling of a spherical steel media in a vibrating bed. Powder Technol 2009;195;2:83-90.
[23] Naeini SE, Spelt JK. Development of single-cell bulk circulation in granular media in a vibrating bed. Powder Technol 2011;1:176-186.
[24] Takahashi Y, Kataoka M, Uekusa M, Terumichi Y. Behavior of Three Kinds of Particles in Rotary Barrel with Planetary Rotation. Multibody Sys Dyn 2005;2:195-209.
[25] Wan S, Sato T, Hartawan A. Vibratory Finishing of Immobilized Cylinders. Adv Mat Res 2012;565:278-283.
[26] Šmilauer V, Catalano E, Chareyre B, Dorofeenko S, Duriez J, Gladky A et al. Yade Reference Documentation. In: Šmilauer V, editor. Yade Documentation, The Yade Project, 1st ed.; 2010;. http://yade-dem.org/doc/.
[27] Hoomans BPB, Kuipers JAM, Briels WJ, van Swaaij WPM: Discrete particle simulation of bubble and slug formation in a two-dimensional gas-fluidised bed: A hard-sphere approach. Chem Eng Sci 1996;1:99-118.
[28] Yuu S, Abe T, Saitoh T, Umekage T. Three-dimensional numerical simulation of the motion of particles discharging from a rectangular hopper using distinct element method and comparison with experimental data. Adv Powder Technol;1995;6;4:259-69.
[29] Thornton C, Cummins SJ, Cleary PW. An investigation of the comparative behaviour of alternative contact force models during elastic collisions. Powder Technol 2011;3:189-97.
[30] Johnstone M. Calibration of DEM models for granular materials using bulk physical tests. Dissertation. Edinburgh: The University of Edinburgh; 2010.
[31] Hertz H. Über die Berührung fester elastischer Körper. J für die Reine und Angewandte Mathematik 1881:156-71.
[32] Mindlin RD. Compilance of Elastic Bodies in Contact. J Appl Mech 1949;20:259-68.
[33] Mindlin RD, Deresiewicz H. Elastic spheres in contact under varying oblique forces. J Appl Mech 1953;20:327-44.
[34] Cundall PA, Strack ODL. A discrete numerical model for granular assemblies. Géotechnique 1979;1:47-65.
[35] Zhang D, Whiten WJ. The calculation of contact forces between particles using spring and damping models. Powder Technol 1996;1:59-64.
[36] Tsuji Y, Tanaka T, Ishida T. Lagrangian numerical simulation of plug flow of cohesionless particles in a horizontal pipe. Powder Technol 1992;3:239-50.
[37] Antypov D, Elliott JA. On an analytical solution for the damped Hertzian spring. EPL 2011;94:1-6.
[38] Grima AP, Wypych PW. Investigation into calibration of discrete element model parameters for scale-up and validation of particlestructure interactions under impact conditions. Powder Technol 2011;1:198-209.
[39] Kumar PP, Sathyan S. Simulation of 1D Abrasive Vibratory Finishing Process. Adv Mat Res 2012;565:290-5.
[40] Hashin Z, Shtrikman S. A variational approach to the theory of the elastic behaviour of multiphase materials. J Mech Phys Solids 1963;2:127-40.
[41] Ondracek G. Zum Zusammenhang zwischen Eigenschaften und Gefügestruktur Mehrphasiger Werkstoffe. Z Werkstofftech 1978;9:96-100.